10/712,247

IFW

Garching Innovation GmbH
Technologien aus der
Max-Planck-Gesellschaft

Hofgartenstraße 8
80539 München
Deutschland
Telefon +49/89/29 09 19-0
Telefax +49/89/29 09 19-99/98
gi@garching-innovation.de
www.garching-innovation.de

Mr. Stuart L. Henderson (Examiner)
Office P/1754
GROUP ART UNIT 1754
U.S. Patent and Trademark Office
220 20th Street South
Crystal Plaza Two, Lobby, Room 1B03
Arlington, VA 22202
USA

Datum: 28. September 2004
Unser Zeichen: BC/ze

Patent Application US 2004-0141906
„Novel graphite nanocatalysts"

Dear Mr. Henderson,

herewith, I would like to draw your attention to two papers, copies attached:

„*Carbon Nanofiliaments in Heterogeneous Catalysis: An Industrial Application for New Carbon Materials*", Mestl et al., Angew. Chem. Int. Ed., 2001, 40, No. 11, pages 2066 to 2125;
(PAPER 1)

„*The Catalytic Use of Onion-Like Carbon Materials for Styrene Synthesis by Oxidative Dehydrogenation of Ethylbenzen*", Keller et al., Angew. Chem. Int. Ed., 2002, 41, No. 11, pages 1885 to 1888. (PAPER 2)

We, the GARCHING INNOVATION, are responsible for the technology transfer of the Max Planck Society. In this function I was approached by the authors of the above articles. They printed out to me that both paper are relevant for the patent application US 2004/0141906. When studying the patent application as well as the papers in greater details we realized the following:

Sitz der Gesellschaft: München
Amtsgericht München HRB 42 363
Vorsitzender des Beirates:
Dr. Axel Ullrich
Geschäftsführer: Dr. Bernhard Hertel
USt-IdNr. DE 129 353382
Steuer-Nr. 812/16706

HypoVereinsbank
BLZ 700 202 70, Kto.-Nr. 041 948 620
Deutsche Bank AG
BLZ 700 700 10, Kto.-Nr. 1 763 994
Postbank
BLZ 700 100 80, Kto.-Nr. 166 020-806

Garching Innovation GmbH
Technologien aus der
Max-Planck-Gesellschaft

Hofgartenstraße 8
80539 München
Deutschland
Telefon +49/89/29 09 19-0
Telefax +49/89/29 09 19-99/98
gi@garching-innovation.de
www.garching-innovation.de

PAPER 1

- This paper published in 2001 already describes the catalytic function of "nanofilaments", "nanofilament walls", "step edges", "inner layer formed by conical graphite layers with an angle of 26° to the filament axis".
- The structure according to Fig. 2 in US '906 ("multifaceted carbon nanotube") and the one stated in the paper ("nanofilaments") are the same.
- As to the dehydrogenation of ethylbenzene to styrene the parameters given in US '906, example 9, page 7 and those in the paper, experimental section on the last page are identical or almost identical, i.e. amount of catalyst, flow, reaction temperatures, temperature for highest yield etc.
- Furthermore, in the text and the scheme on the last page the general "mechanism of the catalytic oxidative dehydrogenation over carbon nanofilaments" is described. The necessary structure of "edges" respectively "step edges" as shown in scheme 1 of the paper is an essential feature for the underlying chemical mechanism. It was first described in the paper in 2001 and is a common feature of all the carbon nanostructures mentioned in US '906.

PAPER 2

- This paper, also being mainly directed towards the catalytic use of Onion-Like Carbon, adds considerable knowledge on the function of "edge/kink sites", "graphitic (0001) facets", "active sites" the tailoring of microstructures " to support the optimum distribution of electron-donating and C-H-activating functions."

We assume that the papers will add useful information to the further examination process.

Sincerely yours,

Garching Innovation GmbH

i.A.

Dr. Bernd Ctortecka

Neue Anschrift ab 18. Oktober:
Marstallstraße 8
80539 München
Tel: 089 / 29 09 19 – 0
Fax: 089 / 29 09 19 – 99
e-mail: gi@garching-innovation.de
www.garching-innovation.de

Sitz der Gesellschaft: München
Amtsgericht München HRB 42 363
Vorsitzender des Beirates:
Dr. Axel Ullrich
Geschäftsführer: Dr. Bernhard Hertel
USt-IdNr. DE 129 353382
Steuer-Nr. 812/16706

HypoVereinsbank
BLZ 700 202 70, Kto.-Nr. 041 948 620
Deutsche Bank AG
BLZ 700 700 10, Kto.-Nr. 1 763 994
Postbank
BLZ 700 100 80, Kto.-Nr. 166 020-806

The Catalytic Use of Onion-Like Carbon Materials for Styrene Synthesis by Oxidative Dehydrogenation of Ethylbenzene

Nicolas Keller, Nadezhda I. Maksimova, Vladimir V. Roddatis, Michael Schur, Gerhard Mestl,* Yurii V. Butenko, Vladimir L. Kuznetsov, and Robert Schlögl*

Since the discovery of fullerenes in 1985,[1] the chemistry of sp^2-hybridized nanostructured carbon has received increasing attention both from a fundamental point of view and for potential applications. A large variety of new fullerene-related materials (giant fullerenes, nanotubes, nanospheres, nanocones, nanofolders, nanobundles, onion-like carbons (OLCs)) have been synthesized.[2] Their unique chemical and physical properties suggest novel applications, which include nanoscale engineering and electronics, optoelectronic sensors; three-dimensional composite-materials, microfilters, magnetic materials, and catalysis.[3] Current research on OLCs is confined to the development of synthesis methods and to the description of physical and chemical properties.[4] These closed, spherical, carbon shells, however, could also provide interesting catalytic properties as a result of the almost perfect graphite network with a high degree of curvature.

Direct dehydrogenation of hydrocarbons is used in numerous industrial processes. Because of their endothermic character, such processes are restricted by thermodynamic limitations, thus alternatives are called for. In case of styrene synthesis, one of the ten most important industrial processes, the exothermic oxidative dehydrogenation (ODH) of ethylbenzene is an elegant and promising reaction, for which carbon catalysts have already proved their efficiency.[5, 6] The porosity of carbon catalysts used to date seems to play a negative role by hindering the styrene desorption. This effect limits the ethylbenzene conversion and leads to nonselective, consecutive reactions.[5, 7] Therefore, because of the absence of inner particle porosity OLCs are valuable candidates as catalysts.[8]

Figure 1 displays the catalytic behavior of the OLC material for the ODH of ethylbenzene to styrene with time on stream (t). For comparison, the steady-state yields are also shown, which were obtained over the industrial K–Fe catalyst and other forms of carbon. The OLC catalyst exhibited a minor initial activity developing into conversion levels of 92% after an activation period of about 2 hours on stream. The stable styrene selectivity of 68% allowed high styrene yields of 62%. The performance of OLC in ODH is not restricted as in case of traditional K-promoted iron-oxide systems, for which thermodynamic constraints limit the maximum styrene yield to 50%.[9, 10]

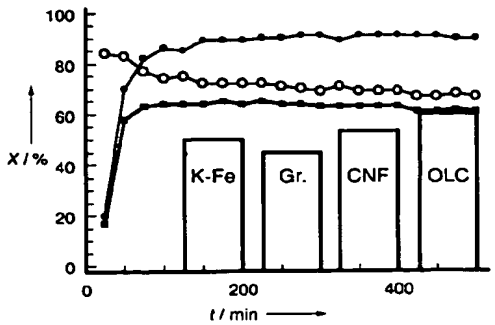

Figure 1. Performance of OLC in the ODH of ethylbenzene at 790 K with time on stream. X = ethylbenzene conversion (●), selectivity to styrene (○), and styrene yield (■). Steady-state styrene yields for graphite (Gr.), carbon nanofilaments $(CNF)_s$ and the industrial K–Fe catalyst are also given. Data are given relative to the catalyst mass.

Figure 2A displays high-resolution transmission electron micrographs of fresh OLC. The left-hand image of Figure 2A shows clean, multishell particles with an interlayer distance close to 0.35 nm, typical for sp^2-hybridized carbon structures. The inset of Figure 2A shows one example of a well resolved OLC. The contrast variations of this OLC indicate not-intact graphene layers and structurally less-defined areas (indicated by arrows) of the curvature. The right-hand image displays OLC material after 40 h catalysis. The OLC seems to have disintegrated into more or less disorganized carbon.

X-ray diffraction (XRD) was further used to characterize the structure of OLC before and after catalysis. Figure 2B shows the XRD data, the diffractogram of fresh OLC is characteristic for graphite-like material with a high degree of stacking faults. For comparison in Figure 2B, the theoretical pattern of hexagonal graphite is indicated by the vertical lines with the respective indexing. The diffractogram recorded after catalysis (Figure 2B, b) demonstrates the generation of diamond-like-carbon (DLC) material, that is, sp^3-hybridized carbon atoms, during the styrene reaction. The peaks at 43.9 and 75.3° 2Θ coincide with the 111 and 220 reflections of diamond as indicated by the vertical lines. Hence, DLC is part of the ill-defined material formed during catalysis.

Figure 2C shows the Raman spectra obtained from the fresh and used OLC. The deconvolution of these spectra is displayed on the right side of Figure 2C. Spectrum (a) exhibits the Raman bands characteristic for disordered (D: 1318 cm^{-1}, and D′: 1602 cm^{-1}) and ordered (G: 1573 cm^{-1} graphene structures.[11] This Raman spectrum is in agreement with the HR-TEM analysis which revealed intact graphene layers and ill-defined structures at the curvatures of OLC (Figure 2A, left) and the XRD data (Figure 2B, pattern a). The intense Raman signature of the D (1328 cm^{-1}) and D′ (1594 cm^{-1}) bands of the catalyst after reaction, completely overwhelming the G band at 1572 cm^{-1} clearly indicate a pronounced presence of disordered carbon structures after the catalytic run. The intensity increase of the two D and D′ Raman signals was accompanied by a broadening and a slight blue-shift of

[*] Prof. Dr. R. Schlögl, Dr. N. Keller, N. I. Maksimova, Dr. V. V. Roddatis, Dr. M. Schur
Abteilung Anorganische Chemie
Fritz-Haber-Institut der Max-Planck-Gesellschaft
Faradayweg 4–6, 14195 Berlin (Germany)
Fax: (+49) 30-8413-4401
E-mail: Schloegl@fhi-berlin.mpg.de
Dr. G. Mestl
Nanoscape AG
Frankfurter Ring 193A, 80809 Munich (Germany)
Dr. Y. V. Butenko, Dr. V. L. Kuznetsov
Boreskov Institute of Catalysis
Lavrentieva 5, 630090 Novosibirsk (Russian Federation)

  1433-7851/02/4111-1885 $ 20.00+.50/0

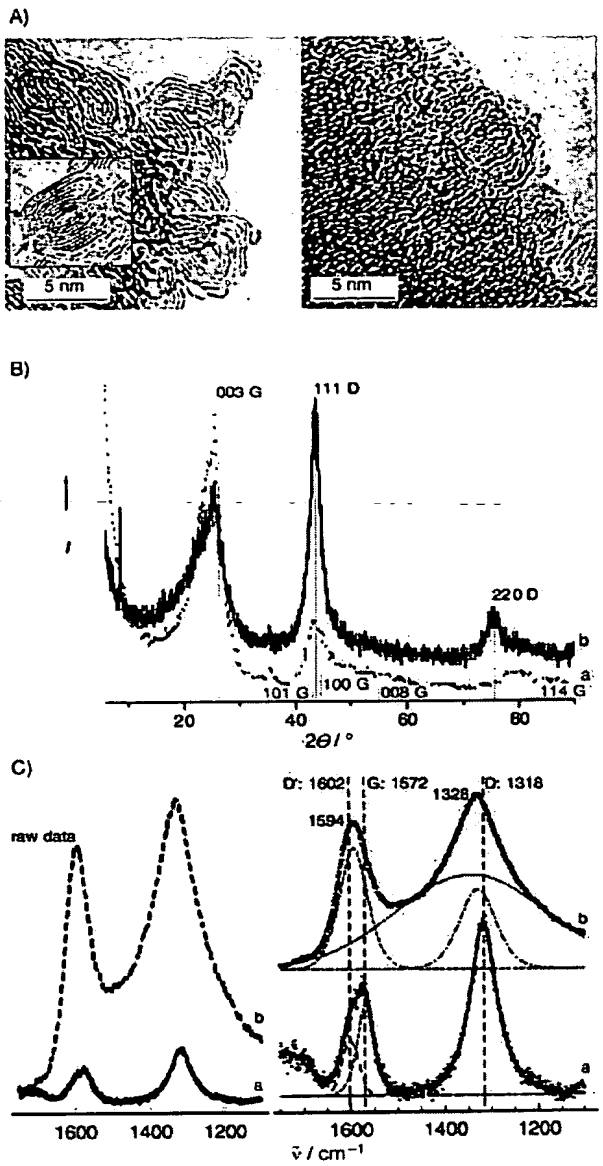

Figure 2. A) High-resolution (HR) TEM images of OLC prior (left) and subsequent to use in the ODH of ethylbenzene (right). The inset shows an enlargement of a single, intact OLC. The arrows indicate the blurred regions with less-ordered structure. B) X-ray diffractograms of the OLC material prior (a) and subsequent to catalysis (b); the calculated positions of the reflections of graphite (G) and diamond (D) are shown. C) Left: original Raman spectra (raw data) of OLC prior (a) and subsequent to use in the ODH of ethylbenzene (b); right: deconvolutions of the Raman spectra prior (a) and subsequent to catalysis (b).

the D band. The deconvolution additionally revealed a very broad background contribution to this band from C–H, C–C deformations.[12] This very broad D band does not exclude the presence of sp^3-hybridized carbon atoms after the reaction, as indicated by XRD (Figure 2B, pattern b).[12] Indeed, IR spectroscopy (spectra not shown) revealed the presence of C–H valence bands at 2920 cm^{-1} after catalysis, together with bands at 1740, 1175, and 1090 cm^{-1} which indicate the presence of basic C=O and C–O groups, respectively.

In addition to Raman spectroscopy and XRD, thermogravimetry temperature-programmed oxidation (TG-TPO) confirmed the presence of these two carbon species (Figure 3). Compared to the fresh, well-organized sp^2-hybridized OLC (Figure 3, curve a), the used catalyst displayed a

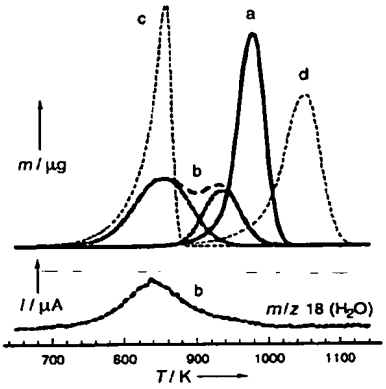

Figure 3. Differential thermal gravimetry of the temperature-programmed combustion of OLC prior (a), subsequent to use in the ODH of ethylbenzene (b), T = temperature, from amorphous carbon (c; Norit A, Aldrich), and graphite (d; SFG6, Timcal AG). Below: mass spectrometer trace of water formed during the combustion of OLC following catalysis.

composite signal (Figure 3, curve b), which indicated disordered sp^2/sp^3-hybridized carbon with a maximum combustion rate at around 850 K, in agreement with the reference sample, amorphous activated charcoal. The contribution to combustion at higher temperatures was assigned to remaining ordered sp^2-carbon structures. The water release, also at 850 K, was detected by mass spectroscopy (Figure 3, bottom) and confirmed the presence of hydrogen atoms (as indicated by IR spectroscopy) in the highly disordered carbon array.

Figure 4 shows the O1s and C1s (X-ray photoemission) XP spectra of fresh and used OLC samples. The almost oxygen-free carbon surface of the fresh OLC (Figure 4A, solid line) was transformed after reaction into an oxygen-containing surface (open circles, Figure 4A). The O1s spectrum after reaction can be deconvoluted into two signals. The first, with a binding energy (B.E.) of 530.9 eV,[13] is similar to spectra reported for other active carbon catalysts[6, 8] and is assigned to chinoidic carbonyl functions. The dehydrogenating power of the catalyst thus seems to be linked to the generation of these strongly basic sites during activation. The second with a B.E. of 533.4 eV arises from water adsorbed during transport through air. Through an increased intensity at the high-energy side of the C1s signal, the C1s spectra (Figure 4B) also indicate the presence of oxidized carbon. The inset of Figure 4B shows the difference spectrum of used OLC (full line) and fresh OLC (dotted line). Its deconvolution confirmed the presence two contributions, at 288.2, indicative for basic, chinoidic surface groups, and 286.0 eV from C–O groups. This XPS finding is in agreement with the IR spectroscopy observations mentioned above. Additionally,

  1433-7851/02/4111-1886 $ 20.00+.50/0

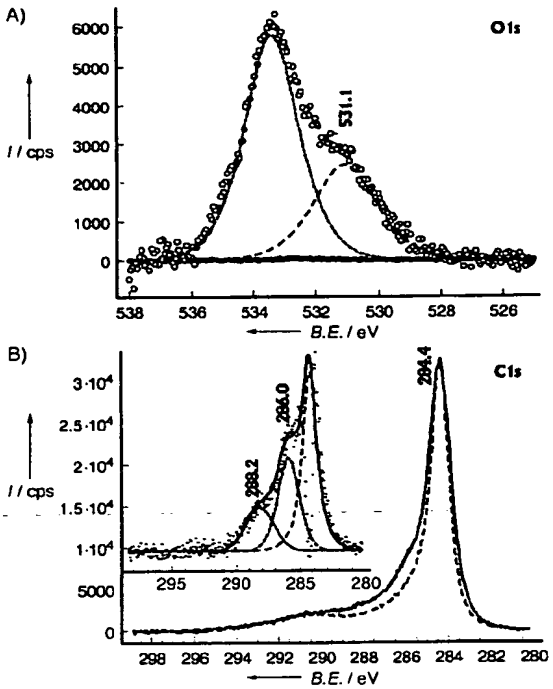

Figure 4. A) O1s XP spectra of the OLC prior (solid line) and subsequent (open circles) to catalysis. The deconvolution into two contributions with B.E. of 531.1 and 533.4 eV is shown. B) C1s XP spectra of OLC prior (dashed line) and subsequent to catalysis (full line). The inset shows the deconvolution of the difference C1s spectrum into three contributions with BE of 288.2, 286.0, and 284.4 eV.

the graphitic C1s line at 284.4 eV was considerably broadened after catalysis demonstrating the presence of structurally ill-defined carbon in line with Raman, XRD, and TG-TPO results

The structural characterization reveals that the function of the OLC as an ODH catalyst is uniquely related to its microstructure. The starting material, intact OLC with a large surface abundance of graphitic (0001) facets combined with a small abundance of edge/kink sites where the bending of the graphene layers occurs (blurred contrast in the TEM, Figure 2), is characterized by the complete absence of surface oxygen functionalities. This material does not show any catalytic activity. Catalytic activity develops with time on stream. The XP spectra indicate the generation of strongly basic, chinoidic surface functionalities on the active carbon catalyst which are responsible for the catalytic activity. These basic, dehydrogenating, surface groups are generated as resonance-stabilized C=O surface terminations of the edge/kink regions of OLC.[7] This oxidation of the edge/kink sites is also seen as being responsible for the disintegration of the OLC during catalysis. The catalytic activity develops with increasing formation of these basic functionalities and accordingly increasing OLC disintegration. Hence, it may be questioned whether OLCs are catalytically active at all. Comparative experiments with ultradispersed diamond (UDD), however, revealed that the DLC material detected by XRD after catalysis can not account for the catalytic activity of OLC (data not shown). UDD are initially also completely inactive, like OLC, but their selectivity, which develops with time, is different from that of OLC; with UDD the main product from the ODH of ethylbenzene is benzene.

That the OLC is superior in its performance to other forms of carbon (Figure 1) indicates that this type of carbon contains a higher number of active sites per unit weight at steady state. This superior performance is also related to the optimized distribution of the oxygen-activating sites (basal planes) and Brønsted basic centers (prismatic planes).[9] The presence of disordered, sp^2- and sp^3-hybridized polymeric carbon resulting from unwanted styrene polymerization is characteristic of all the catalytic systems tested so far.[9, 14] However the large volume and great number of defects in such polymeric (amorphous) species, makes them particularly susceptible to oxidation in situ (see Figure 3). As the formation of coke cannot be completely avoided a large difference in specific reactivity of the soft coke (polymeric species)[15] and the carbon catalyst is a prerequisite for stable operation. Reducing the number of basic sites, which cause polymerization, to the minimum necessary for activating the ethylbenzene substrate, makes the tendency for coke formation on carbon lower than on (potassium-promoted) metal-oxide systems.

The results reveal that a significant potential for catalytic application lies in unpromoted nanocarbon materials if their microstructure can be tailored to support the optimum distribution of electron-donating and C–H-activating functions. The chemical simplicity of carbon and the unique self-cleaning property that deactivated surfaces gasify themselves in ODH reactions, not only makes carbon species well-suited model systems but also allows realistic expectations of an industrial application in heterogeneous catalysis. The difficulties associated with the synthesis of the present OLC model system may be overcome by tailoring other more abundant forms of carbon into the desired target structure by synthetic[16] and post-synthetic thermochemical procedures.

Experimental Section

OLCs were produced by thermal annealing of UDD powder at 2140 K under a 10^{-6} torr vacuum, according to ref. [17]. The reaction was carried out in a tubular quartz reactor of 4 mm inner diameter and 200 mm length. The catalyst (0.04 g) was placed in the isothermal oven zone between quartz wool plugs. He and O_2 were fed by mass-flow controllers (Bronkhorst). Ethylbenzene in a stream of He was provided by a saturator kept at the required temperature (35 °C, corresponding to 2.16 kPa) and mixed with the O_2 flow to obtain the ethylbenzene:O_2 ratio of 1:1. The reaction was conducted at 790 K with an inlet ethylbenzene concentration of 2 vol % and a liquid hourly space velocity (LHSV) of 0.5 h^{-1}. The inlet and outlet gas analysis was carried out online by a gas chromatograph using a packed column (5 % SP-1200/1.75 % Bentone 34) for hydrocarbons and a capillary column (Carboxen 1010 PLOT) for permanent gases coupled to a flame ionization detector (FID) and a thermal conductivity detector (TCD), respectively.

TEM micrographs were taken on a Phillips CM200-FEG at an acceleration voltage of 200 kV. XP spectra were recorded with a modified Leybold Heraeus spectrometer (LHS12 MCD) with $Mg_{K\alpha}$ radiation (1253.6 eV) at a power of 240 W. The bandpass energy was set to 50 eV. X-ray satellites and Shirley background were subtracted. Thermal gravimetry analysis was performed on a Netzsch STA 449C balance, with a heating rate of 10 K min^{-1} and by using a 20 % (v/v) O_2/He mixture, and coupled to a QMS200 mass spectrometer (Thermostar, Pfeiffer Vacuum). Raman spectra were recorded with a LabRam spectrometer (Dilor). The slit width

was set at 500 μm giving a spectral resolution of 5 cm^{-1}. A He/Ne laser at 632.8 nm was used as the excitation source. IR spectra in diffuse reflectance were recorded on a Bruker IFS-66 FT-IR spectrometer. XRD was performed on a Stoe Theta-Theta diffractometer in reflection ($Cu_{K\alpha}$ radiation).

Received: July 23, 2001
Revised: March 5, 2002 [Z17567]

[1] H. W. Kroto, J. R. Heath, S. C. O'Brien, R. F. Curl, R. E. Smalley, *Nature* **1985**, *318*, 162.
[2] a) S. Iijima, *Nature* **1991**, *354*, 56; b) D. Ugarte, *Nature* **1992**, *359*, 670; c) H. O. Pierson, *Handbook of Carbon, Graphite, Diamond and Fullerenes. Properties, Processing and Applications*, Noyes Publications, Park Ridge, **1993**; d) M. Jose-Yacamau, H. Terrones, L. Rendou, J. M. Dominguez, *Carbon* **1995**, *33*, 669; e) *Carbon nanotubes: preparation and properties* (Ed.: T. W. Ebbesen), CRC, Boca Raton, **1997**; f) M. Knupfer, *Surf. Sci. Rep.* **2001**, *42*, 1, and references therein.
[3] a) M. Terrones, W. Kuang Hsu, H. W. Kroto, D. R. M. Walton, *Top. Curr. Chem.* **1999**, *199*, 189, and references therein; b) P. M. Ajayan, O. Z. Zhou *Top. Appl. Phys.* **2001**, *80*, 391.
[4] a) D. Ugarte, *Carbon* **1995**, *33*, 989; b) V. L. Kuznetsov, Yu. V. Butenko, A. L. Chuvilin, A. I. Romanenko, A. V. Okotrub, *Chem. Phys. Lett.* **2001**, *336*, 397.
[5] M. F. R. Pereira, J. J.M Orfao, J. L. Figueiredo, *Appl. Catal. A* **1999**, *184*, 153.
[6] G. Mestl, N. I. Maksimova, N. Keller, V. V. Roddatis, R. Schlögl, *Angew. Chem.* **2001**, *113*, 2122; *Angew. Chem. Int. Ed.* **2001**, *40*, 2066.
[7] a) C. Kuhrs, Y. Arita, W. Weiss, W. Ranke, R. Schlögl, *Top. Catal.* **2001**, *14*, 111; b) J. A. Maciá, D. C. Amorós, A. L. Solano, *Proceedings of the Reunión de la Sociedad Española de Catálisis*, **2001**, pp. 97–98.
[8] a) A more detailed comparison of the performances obtained with different forms of carbon will be given in a coming extended paper; b) storage in air and transfer to the XPS chamber led to a second contribution arising from adsorbed water.
[9] G. Emig, H. Hofmann, *J. Catal.* **1983**, *84*, 15.
[10] F. Cavani, F. Trifiro, *Appl. Catal. A* **1995**, *133*, 219.
[11] a) R. P. Vidano, D. B. Fishbach, L. J. Willis, T. M. Loehr, *Solid State Commun.* **1981**, *39*, 423; b) M. S. Dresselhaus, G. Dresselhaus, *Adv. Phys.* **1981**, *30*, 139; c) Y. Kawashima, G. Katagiri, *Phys. Rev. B* **1995**, *52*, 10053.
[12] D. Espinat, H. Dexpert, E. Freund, G. Martino, M. Couzi, P. Lespade, F. Cruege, *Appl. Catal.* **1985**, *16*, 343.
[13] a) H. Ago, T. Kugler, F. Cacialli, W. R. Salaneck, M. S. P. Shaffer, A. H. Windle, R. H. Friend, *J. Phys. Chem. B* **1999**, *103*, 8116; b) M. Voll, H. P. Boehm, *Carbon* **1971**, *9*, 481.
[14] G. E. Vrieland, *J. Catal.* **1988**, *111*, 14.
[15] R. Schlögl in *Handbook of Heterogeneous Catalysis, Vol. 1* (Eds.: G. Ertl, H. Knözinger, J. Weitkamp), Wiley-VCH, Weinheim, **1997**, pp. 138–191.
[16] C. Pham-Huu, N. Keller, V. V. Roddatis, G. Mestl, R. Schlögl, M. J. Ledoux, **2002**, *4*, 514–521.
[17] a) V. L. Kuznetsov, A. L. Chuvilin, Yu. V. Butenko, I. Y. Mal'kov, V. M. Titov, *Chem. Phys. Lett.* **1994**, *222*, 343; b) V. L. Kuznetsov, A. L. Chuvilin, E. M. Moroz, V. N. Kolomiichuk, Sh. K. Shaikhutdinov, Yu. V. Butenko, *Carbon* **1994**, *32(5)*, 873.

Tin Analogues of "Arduengo Carbenes": Synthesis of 1,3,2λ^2-Diazastannoles and Transfer of Sn Atoms between a 1,3,2λ^2-Diazastannole and a Diazadiene**

Timo Gans-Eichler, Dietrich Gudat,* and Martin Nieger

The discovery of persistent and in preparative-scale isolable carbenes launched not only a rapid development of carbene chemistry,[1] but stimulated as well investigations on carbene homologues with heavier Group 14 elements. Utilization of the concept that mesomeric interaction with the π electrons of two nitrogen atoms and a C–C double bond allows efficient electronic stabilization of the divalent carbon atom in imidazoyl ("Arduengo-type") carbenes **I**[2] lead to the isolation of analogous silylenes **II**;[3] and germylenes **III** (Scheme 1).[4] Homologues of **I** with Sn (**IV**) and Pb (**V**) are—apart from a few annellated 1,3,2λ^2-diazastannoles[5]—still unknown, although divalent compounds of these elements should become increasingly more stable descending the group from C to Pb.[6] We report here the preparation and first reaction studies of monocyclic 1,3,2λ^2-diazastannoles **IV** which reveal that the reactivity of these compounds displays some striking dissimilarities when compared to the lighter homologues **I**–**III**.

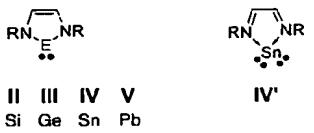

I **II** **III** **IV** **V** **IV'**
E = C Si Ge Sn Pb

Scheme 1.

λ^2-Diazagermoles **III** and annellated λ^2-diazastannoles can be prepared by metathesis of dilithiated diazadienides or *o*-phenylene diamides with $GeCl_2 \cdot$dioxane or $SnCl_2$, respectively.[4, 5] Analogous reactions of $SnCl_2$ with the dilithiumdiamides **2a, b** (Scheme 2) failed,[7] but the desired monocyclic diazastannoles **7a,b** were found to be accessible by transamination of the α-amino aldimines **3a,b**[8] with $[Sn(N(SiMe_3)_2)_2]$ (**4**) at 40–45 °C in nonpolar solvents. Mechanistically, the formation of **7a,b** can be explained by a multistep sequence (Scheme 2) which involves the initial condensation of **3a,b** and **4** to give stannylenes **5**, a subsequent 1,3-H-shift to afford **6**, and finally intramolecular elimination of $HN(SiMe_3)_2$ to produce the final products **7a,b** which were isolated after workup as red, air sensitive, and rather thermolabile solids. Experimental support for this

[*] Prof. Dr. D. Gudat, Dipl.-Chem. T. Gans-Eichler, Dr. M. Nieger
Institut für Anorganische Chemie
Universität Bonn
Gerhard-Domagk Strasse 1, 53121 Bonn (Germany)
Fax: (+49) 228-73-5327
E-mail: dgudat@uni-bonn.de

[**] This work was supported by the Deutsche Forschungsgemeinschaft. Parts were presented as a poster at the Jahrestagung Chemie 2001 der GDCH.

  1433-7851/02/4111-1888 $ 20.00+.50/0

[1] a) S. Rowan, D. E. Fisher, *Leukemia* **1997**, *11*, 457–465; b) P. H. Krammer, *Adv. Immunol.* **1998**, *71*, 164–210; c) A. Ashkenazi, V. M. Dixit, *Science* **1998**, *281*, 1305–1308; d) P. Wehrli, I. Viard, R. Bullani, J. Tschopp, L. E. French, *J. Invest. Dermatol.* **2000**, *115*, 141–148; e) T. Herget, *Nachr. Chem. Tech. Lab.* **2001**, *49*, 328–330; f) U. Sartorius, I. Schmitz, P. H. Krammer, *ChemBioChem* **2001**, *2*, 20–29.

[2] A. M. Danen-Van Oorschot, D. F. Fischer, J. M. Grimbergen, B. Klein, S.-M. Zhuang, J. H. F. Falkenburg, C. Backendorf, P. H. A. Quax, A. J. Van der Eb, H. M. Noteborn, *Proc. Natl. Acad. Sci. USA* **1997**, *94*, 5843–5847.

[3] a) Y. Hayakawa, J. W. Kim, H. Adachi, K. Shin-ya, K. Fujita, H. Seto, *J. Am. Chem. Soc.* **1998**, *120*, 3524–3525; b) J. W. Kim, H. Adachi, K. Shin-ya, Y. Hayakawa, H. Seto, *J. Antibiot.* **1997**, *50*, 628–630.

[4] a) A. R. Salomon, Y. Zhang, H. Seto, C. Khosla, *Org. Lett.* **2001**, *3*, 57–59; b) A. R. Salomon, D. W. Voehringer, L. A. Herzenberg, C. Khosla, *Chem. Biol.* **2001**, *8*, 71–80.

[5] a) J. Schuppan, B. Ziemer, U. Koert, *Tetrahedron Lett.* **2000**, *41*, 621–624; b) K. C. Nicolaou, Y. Li, B. Weyershausen, H.-X. Wei, *Chem. Commun.* **2000**, 307–308; c) G. A. Sulikowski, W.-M. Lee, B. Jin, B. Wu, *Org. Lett.* **2000**, *2*, 1439–1442.

[6] Since the hydroxy group at C20 is sterically hindered, lactonization should occur with the hydroxy group at C19. See also: a) R. B. Woodward, E. Logusch, K. P. Nambiar, K. Sakan, D. E. Ward, B.-W. Au-Yeung, P. Balaram, L. J. Browne, P. J. Card, C. H. Chen, R. B. Chênevert, A. Fliri, K. Frobel, H.-J. Gais, D. G. Garratt, K. Hayakawa, W. Heggie, D. P. Hesson, D. Hoppe, I. Hoppe, J. A. Hyatt, D. Ikeda, P. A. Jacobi, K. S. Kim, Y. Kobuke, K. Kojima, K. Krowicki, V. J. Lee, T. Leutert, S. Malchenko, J. Martens, R. S. Matthews, B. S. Ong, J. B. Press, T. V. Rajan Babu, G. Rousseau, H. M. Sauter, M. Suzuki, K. Tatsuta, L. M. Tolbert, E. A. Truesdale, I. Uchida, Y. Ueda, T. Uyehara, A. T. Vasella, W. C. Vladuchick, P. A. Wade, R. M. Williams, H. N.-C. Wong, *J. Am. Chem. Soc.* **1981**, *103*, 3213–3215; b) M. Kageyama, T. Tamura, M. H. Nantz, J. C. Roberts, P. Somfai, D. C. Whritenour, S. Masamune, *J. Am. Chem. Soc.* **1990**, *112*, 7407–7408.

[7] B. Tse, *J. Am. Chem. Soc.* **1996**, *118*, 7094–7100.

[8] B. H. Lipshutz, R. Keil, E. L. Ellsworth, *Tetrahedron Lett.* **1990**, *31*, 7257–7260.

[9] Bromide **11** was prepared from the corresponding alcohol as follows: 1) MsCl, Et_3N, 2) LiBr, acetone (Ms = mesyl = methanesulfonyl). See: V. Fargeas, P. L. Ménez, I. Berque, J. Ardisson, A. Pancrazi, *Tetrahedron* **1996**, *52*, 6613–6634.

[10] M. T. Reetz, *Angew. Chem.* **1984**, *96*, 542–555; *Angew. Chem. Int. Ed. Engl.* **1984**, *23*, 556–569.

[11] M. Larcheveque, S. Henrot, *Tetrahedron* **1987**, *43*, 2303–2310.

[12] D. B. Dess, J. C. Martin, *J. Org. Chem.* **1983**, *48*, 4155–4156.

[13] K. Takai, T. Ichiguchi, S. Hisaka, *Synlett* **1999**, *8*, 1268–1270.

[14] The light sensitivity of **18** is under current investigation. Upon irradiation at 365 nm, the absorption band at 295 nm decreased. Concomittantly an increase at about 240 nm is observed.

[15] a) J. K. Stille, *Angew. Chem.* **1986**, *98*, 504–519; *Angew. Chem. Int. Ed. Engl.* **1986**, *25*, 508–523; b) T. N. Mitchell, *Synthesis* **1992**, 803–815; c) I. Paterson, V. A. Doughty, M. D. McLeod, T. Trieselmann, *Angew. Chem.* **2000**, *39*, 1364–1368; *Angew. Chem. Int. Ed.* **2000**, *39*, 1308–1312.

[16] a) G. D. Allred, L. S. Liebeskind, *J. Am. Chem. Soc.* **1996**, *118*, 2748–2749; b) I. Paterson, H.-G. Lombart, C. Allerton, *Org. Lett.* **1999**, *1*, 19–22.

[17] a) J. Inanaga, K. Hirata, H. Saeki, T. Katsuki, M. Yamaguchi, *Bull. Chem. Soc. Jpn.* **1979**, *52*, 1989–1993; b) D. A. Evans, D. M. Finch, T. E. Smith, V. J. Cee, *J. Am. Chem. Soc.* **2000**, *122*, 10033–10046.

[18] Analytical data (R_f and $[\alpha]_D$ values, IR, ^1H and ^{13}C NMR, and HR mass spectra) of **12**, **18**, **20**, **21**, and apoptolidinone are available in the Supporting Information.

Carbon Nanofilaments in Heterogeneous Catalysis: An Industrial Application for New Carbon Materials?**

Gerhard Mestl, Nadezhda I. Maksimova, Nicolas Keller, Vladimir V. Roddatis, and Robert Schlögl*

The direct dehydrogenation of ethylbenzene to styrene is one of the ten most important industrial processes. In this process a potassium-promoted iron catalyst is used at temperatures between 870 and 930 K.[1] However, this method is thermodynamically limited and, because of the required excess of steam, very energy consuming.[2, 3] The oxidative dehydrogenation (ODH) of ethylbenzene could be a promising alternative in which the hydrogen generated is directly oxidized making the overall process exothermic.

Mechanistic studies of the dehydrogenation of ethylbenzene on single-crystal model surfaces provide fundamental information about the role of the active K–Fe phase.[4–7] This surface is evidently well suited to generate a graphitic carbon deposit. Therefore, it is possible that these carbon deposits are actually the catalytically active phase.

Transition metal oxides[8] and phosphates[9, 10] as well as polymers[11] have been described as active and selective catalysts for the ODH of ethylbenzene. The carbon deposits[12] detected on such catalysts again point to an active role of carbon in this reaction. Accordingly, catalytic activity in the ODH was demonstrated for activated charcoals,[13, 14] their commercialization however, is impossible because of their low oxidation resistance.[15] Graphite, on the other hand, exhibits activity in the ODH of methanol.[16] Thus, graphitic carbon materials, that is, nanofilaments with high surface area, are promising candidates for dehydrogenation catalysts in the presence of oxygen.

We have tested the catalytic properties of lamp soot, graphite, and nanofilaments for the ODH of ethylbenzene to styrene. Figure 1 displays the catalytic properties of the investigated carbon materials with time on stream *t*. The higher activity of nanofilaments relative to soot and graphite is evident. While the catalytic activity of soot decreases during the induction period because of burn-off, that of graphite and the nanofilaments increases with time. This behavior can be correlated with the stability toward combustion. Nanofilaments show a higher activity, selectivity, and yield relative to graphite. The catalytic properties of the three investigated carbon materials after 7 h operation are given in Table 1. Again the superiority of the nanofilaments over graphite is evident. Although the specific activity of nanofilaments is somewhat lower, they exhibit comparable selectivity and

[*] Prof. Dr. R. Schlögl, Dr. G. Mestl, N. I. Maksimova, Dr. N. Keller, Dr. V. V. Roddatis
Abteilung Anorganische Chemie
Fritz-Haber-Institut der Max-Planck-Gesellschaft
Faradayweg 4–6, 14195 Berlin (Germany)
Fax: (+49) 30-8413-4401
E-mail: Schloegl@fhi-berlin.mpg.de

[**] We thank the TIMCAL AG (Switzerland) for the generous provision of the graphite.

  1433-7851/01/4011-2066 $ 17.50+.50/0

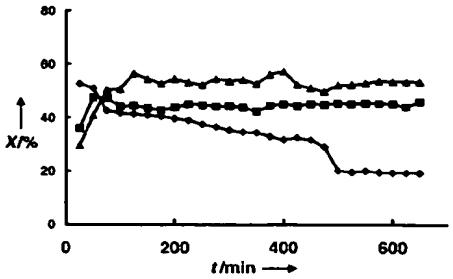

Figure 1. The styrene yield from soot (◆), graphite (■), and nanofilaments (▲) with time on stream in the oxidative dehydrogenation of ethylbenzene at 820 K.

Table 1. Comparison of the specific activities, selectivities, and yields of styrene, and the specific surface areas of lamp soot,[a] graphite, and nanofilaments after 7 h reaction.

Catalyst	Lamp soot[a]	Graphite	Filaments
Spec. activity [10^{-7} mol m^{-2}]	(14.40)	3.66	3.03
Selectivity [%]	(65)	80	85
Spec. yield [10^{-7} mol m^{-2}]	(9.32)	2.93	4.67
Spec. surface area [$m^2 g^{-1}$]	(19)	69	47

[a] Values in parentheses indicate that Lamp soot quantitatively combusts under the reaction conditions.

hence a 37% higher specific yield of styrene. After 7 h operation, soot still shows good performance but with extended time on stream burns up completely under these reaction conditions.

Figure 2 displays two high resolution transmission electron micrographs of nanofilament walls before and after the reaction. The fresh nanofilament walls (Figure 2a) are built

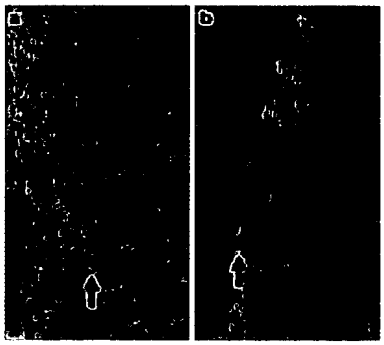

Figure 2. High resolution TEM images of the walls of carbon nanofilaments before (a) and after (b) the oxidative dehydrogenation of ethylbenzene. Arrows mark the boundary layer between the conical graphite layers and the outer shell.

up by two different layers. The inner layer is formed by conical graphite layers with an angle of 26° to the filament axis. The interlayer distance of 0.348 nm is comparable to that of normal graphite. The outer nanofilament shell is formed by ill-defined carbon layers which are oriented parallel to the filament axis. The mean layer distance is about 0.388 nm. After the catalytic reaction, the nanofilaments have an altered wall structure (Figure 2b): the outer shell of ill-defined carbon layers is combusted and a thin layer of polymeric carbon deposits covers the outer surface of the conical graphite layers. This carbon deposit can be seen especially at the step edges between the conical layers. Additionally, the ends of the conical layers seem to be partially oxidized. These partially oxidized prism faces presumably play an important role in the catalytic reaction.

The purity and composition of the test materials was characterized prior to catalysis by X-ray photoemission spectroscopy (XPS) and energy dispersive X-ray spectroscopy (EXD). The ratio of graphitic to aliphatic carbon was determined to be 0.13:1 for soot, 0.19:1 for graphite, and 0.15:1 for the nanofilaments. Hence, within the experimental error, this ratio is the same for all samples. The oxygen content was determined by EDX to be 10–20 wt% for all samples. Thus within the experimental error no difference in the oxygen content of the samples could be determined. The remaining iron-catalyst particles in the nanofilaments were always completely covered by carbon and clearly could not play an active part in the reaction.

Figure 3 displays the O(1s) XP spectrum of the nanofilament catalyst after ODH. Among others a very weak signal can be seen at 530.2 eV [17] which points to the presence of

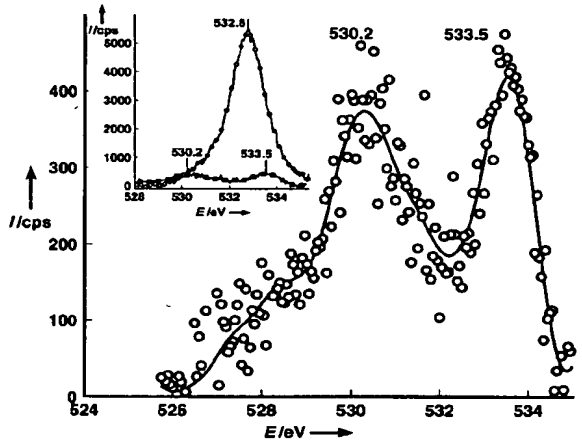

Figure 3. O(1s) XP spectrum of the carbon nanofilaments after oxidative dehydrogenation of ethylbenzene. The inset shows a comparison of the spectra before (○) and after (■) the catalytic reaction.

strongly basic surface oxygen groups,[17] for example, quinoidic groups.[18] Another weak signal at 533.6 eV is attributed to adsorbed water.[19] The detection of strongly basic groups after the catalytic reaction indicates the important dehydrogenating function these groups have during the catalytic process.

A possible reaction mechanism of the ODH of ethylbenzene over nanofilaments is shown in Scheme 1. Strongly basic, adjacent (quinoidic) oxygen centers dehydrogenate ethylbenzene to styrene under the formation of surface OH groups.[3, 9, 20] Gas-phase oxygen is dissociated on the basal planes of the graphite layers[16] and diffuses to the hydroxyl groups, which then react under reformation of the quinoidic groups and the desorption of water.

  1433-7851/01/4011-2067 $ 17.50+.50/0

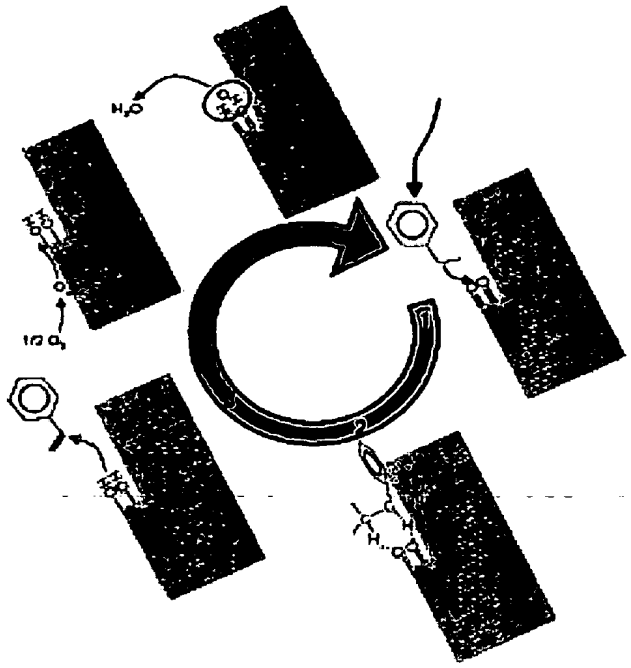

Scheme 1. Mechanism of the catalytic oxidative dehydrogenation over carbon nanofilaments, 1) adsorption of ethylbenzene, 2) dehydrogenation at basic centers, 3) desorption of styrene, 4) adsorption of oxygen and reaction with OH groups, 5) desorption of water.

Catalytic ODH giving good yields seems to be possible over carbon catalysts. Carbon nanofilaments in particular display a high stability toward oxidation; their recently reported cheap synthesis by catalytic decomposition[21] seems to make a first industrial application of carbon nanofilaments plausible. Rational design of experiments on the basis of a functional analysis of industrial catalysts with the aid of surface-science methods resulted, in a short time, in a high-temperature stable, active, and selective catalyst for the ODH of ethylbenzene.

Experimental Section

Soot (Lamp soot 101, Degussa), graphite (HSAG, TIMCAL) and commercial carbon nanofilaments (Applied Science) were used as catalysts for the oxidative dehydrogenation of ethylbenzene to styrene. The reaction was carried out in a tubular quartz reactor, inner diameter 4 mm, length 200 mm. The catalysts (0.02 g) were held in the isothermal oven zone by quartz wool plugs. He and O_2 were fed in by mass flow controllers. Ethylbenzene (EB) was evaporated at 35 °C (2.16 kPa) in a flow of He and mixed with the O_2 flow to obtain different EB:O_2 ratios (0:1, 1:1, 2:1). The reaction was carried out at 820 K in a total flow of 10 mL min^{-1} (LHSV (liquid hourly space velocity): 0.5 h^{-1}). The reaction products were analyzed on-line by gas chromatography (hydrocarbons with a 5% SP-1200/1.75% Bentone 34 packed column and flame ionization detector (FID); permanent gases with a Carboxen 1010 PLOT column/thermal conductivity detector).

The ethylbenzene conversion (X_{EB}), the styrene yield (Y_{ST}) and the selectivity to styrene (S_{ST}) were calculated according the standard reaction engineering Equations (1)–(3).

$$X_{EB} = \frac{n_{EB_0} - n_{EB_{out}}}{n_{EB_0}} \quad (1)$$

$$S_{ST} = \frac{n_{ST}}{n_{EB_0} - n_{EB_{out}}} \quad (2)$$

$$Y_{ST} = \frac{n_{ST}}{n_{EB_0}} \quad (3)$$

To calculate the specific activity, X_{EB} was divided by the catalyst mass and its specific surface area. The specific styrene yield was obtained analogously by dividing Y_{ST} by the catalyst mass and its specific surface area.

Transmission electron microscopy was carried out on a Phillips CM200-FEG at an acceleration voltage of 200 kV. Photoelectron spectra were recorded on a modified Leybold Heraeus spectrometer (LHS12 MCD) with $Mg_{K\alpha}$ radiation (1253.6 eV) and a power of 240 W. The bandpass energy was set to 50 eV. X-ray satellites and Shirley background was subtracted. The Brunauer–Emmett–Teller (BET) surface area of the catalysts was determined by N_2 adsorption at 77 K.

Received: December 27, 2000 [Z16326]

[1] D. H. James, W. M. Castor in *Ullmann's Encyclopedia of Industrial Chemistry, Vol. 25* (Eds.: B. Elvers, S. Hawkins, M. Ravenscroft, G. Schulz), 5. ed., VCH, Weinheim, **1994**, pp. 329–344.
[2] J. Matsui, *Appl. Catal.* **1989**, *51*, 203.
[3] F. Cavani, F. Trifiro, *Appl. Catal. A* **1995**, *133* 219.
[4] M. Muhler, R. Schlögl, G. Ertl, *J. Catal.* **1992**, *138*, 413.
[5] W. Weiss, D. Zscherpel, R. Schlögl, *Catal. Lett.* **1998**, *52*, 215.
[6] Sh. K. Shaikhutdinov, Y. Joseph, C. Kuhrs, W. Ranke, W. Weiss, *Faraday Discuss. Chem. Soc.* **1999**, *114*, 363.
[7] C. Kuhrs, Y. Arita, W. Weiss, W. Ranke, R. Schlögl, unpublished results.
[8] Z. Dziewiecki, A. Makowski, *React. Kinet. Catal. Lett.* **1980**, *13*, 51.
[9] G. Emig, H. Hofmann, *J. Catal.* **1983**, *84*, 15.
[10] G. E. Vrieland, P. G. Menon, *Appl. Catal.* **1991**, *77*, 1.
[11] G. C. Grunewald, R. S. Drago, *J. Mol. Catal.* **1990**, *58*, 227.
[12] W. Ogranowski, J. Hanuza, L. Kepinski, *Appl. Catal. A* **1998**, *171*, 145.
[13] T. G. Alkhazov, *Kinet. Katal.* **1972**, *13*, 509.
[14] M. F. R. Pereira, J. J. M. Orfao, J. L. Figueiredo, *Appl. Catal. A* **1999**, *184*, 153.
[15] M. F. R. Pereira, J. J. M. Orfao, J. L. Figueiredo, *Appl. Catal. A* **2000**, *196*, 43.
[16] R. Schlögl in *Handbook of Heteogeneous Catalysis, Vol. 1* (Eds.: G. Ertl, H. Knözinger, J. Weitkamp), Wiley-VCH, Weinheim, **1997**, pp. 138–191.
[17] H. Ago, T. Kugler, F. Cacialli, W. R. Salaneck, M. S. P. Shaffer, A. H. Windle, R. H. Friend, *J. Phys. Chem. B* **1999**, *103*, 8116.
[18] M. Voll, H. P. Boehm, *Carbon* **1971**, *9*, 481.
[19] Water is absorbed by the hydophilic groups during transfer to the XPS analysis.
[20] G. E. Vrieland, *J. Catal.* **1988**, *111*, 14.
[21] O. P. Krivoruchko, N. I. Maksimova, V. I. Zaikovskii, A. N. Salanov, *Carbon* **2000**, *38*, 1075.

  1433-7851/01/4011-2068 $ 17.50+.50/0